Title Page (Int J Mol Sci)

Inhibition of experimental choroidal neovascularization by a novel peptide derived from calreticulin anti-angiogenic domain

Youn-Shen Bee[1,2,3], Jinying Chen[4,5], Pei-Jhen Tsai[1], Shwu-Jiuan Sheu[1,6,7], Hsiu-Chen Lin[1], Hu Huang[8], Guei-Sheung Liu[4,5,9†] and Ming-Hong Tai[10†]

[1]Department of Ophthalmology, Kaohsiung Veterans General Hospital, Kaohsiung, Taiwan

[2]Yuh-Ing Junior College of Health Care & Management, Kaohsiung, Taiwan

[3]National Defense Medical Center, Taipei, Taiwan

[4]Menzies Institute for Medical Research, University of Tasmania, Hobart, Tasmania, Australia

[5]Department of Ophthalmology, the First Affiliated Hospital of Jinan University, Guangzhou, Guangdong, China

[6]School of Medicine, National Yang-Ming University, Taipei, Taiwan

[7]Department of Medical Education and Research, Kaohsiung Veterans General Hospital, Kaohsiung, Taiwan

[8]Aier Eye Institute; Aier School of Ophthalmology, Central South University, Changsha, Hunan, China

[9]Ophthalmology, Department of Surgery, University of Melbourne, East Melbourne, Victoria, Australia

[10]Department of Biomedical Sciences, National Sun Yat-Sen University, Kaohsiung, Taiwan

[†]These authors contributed equally to this work and should be regarded as equal senior authors.

Running title: Calreticulin-derived peptide inhibits choroidal neovascularization

 doi:10.20944/preprints201807.0347.v1

Correspondence should be addressed to:

Ming-Hong Tai, Ph. D.

Department of Biomedical Sciences, National Sun Yat-Sen University, Kaohsiung, Taiwan. No.70, Lianhai Rd., Kaohsiung City 804, Taiwan

Tel: +886-7-5252000 ext. 5816, FAX: +886-7-3468054,

e-mail: minghongtai@gmail.com

and

Youn-Shen Bee M.D, Ph. D.

Department of Ophthalmology, Kaohsiung Veterans General Hospital, Kaohsiung, Taiwan. No.386, Dazhong 1st Rd., Zuoying Dist., Kaohsiung 81362, Taiwan.

Tel: +886-7-3468217, FAX: +886-7-3468054,

e-mail: ysbee@vghks.gov.tw

Preprints (www.preprints.org) | NOT PEER-REVIEWED | Posted: 19 July 2018 doi:10.20944/preprints201807.0347.v1

ABSTRACT

Choroidal neovascularization (CNV) is a key pathological feature of several of the leading causes of vision loss including neovascular age-related macular degeneration. Here we show that a calreticulin anti-angiogenic domain (CAD)-like peptide 27, CAD27, inhibited *in vitro* angiogenic activities, including tube formation and migration of endothelial cells, and suppressed vascular sprouting from rat aortic ring explants. In rat model of laser-induced CNV, we demonstrate that intravitreal injection of CAD27 significantly attenuated the formation of CNV lesions as measured via fundus fluorescein angiography and choroid flat-mounts (19.5% and 22.4% reductions at 10μg and 20μg of CAD27 injected, respectively). Similarly, the reduction of CNV lesions was observed in the groups of rats that had received topical applications of CAD27 (choroid flat-mounts: 17.9% and 32.5% reductions at 10μg/mL and 20μg/mL of CAD27 installed, respectively). Retinal function was unaffected, as measured using electroretinography in both groups received interareal injection or topical applications of CAD27 at least for 9 days. These findings show that CAD27 can be used as a potential therapeutic alternative for targeting CNV in the diseases such as neovascular age-related macular degeneration.

Keywords: choroidal neovascularization; neovascular age-related macular degeneration; calreticulin anti-angiogenic domain.

Preprints (www.preprints.org) | NOT PEER-REVIEWED | Posted: 19 July 2018 doi:10.20944/preprints201807.0347.v1

INTRODUCTION

Choroidal neovascularization (CNV) is the primary cause for vision loss in patients with wet (exudative or neovascular) age-related macular degeneration (nAMD; see review in ref[1]) and degenerative myopia (see review in ref[2]). In these conditions, abnormally high levels of vascular endothelial growth factor (VEGF) are secreted. VEGF causes the pathological formation of blood vessels in the eye but also leads to leakage of blood and fluid into the eye, damaging the retina and leading to vision loss. The recent availability of anti-VEGF therapies (VEGF-neutralizing proteins, such as monoclonal antibodies, antibody fragments and antibody-receptor fusion proteins) has revolutionized the treatment of choroidal neovascularization by preserving and even restoring vision in patients[3, 4]. However, existing anti-VEGF therapeutics are expensive and require frequent intravitreal injections (often for many years) to achieve therapeutic benefit. Moreover, a lack of capacity for repeated injections in the public health system may also pose a barrier to access for patients. Thus, there is a need to seek cost-effective and less-invasive and more durable alternative therapies for these conditions.

The calreticulin anti-angiogenic domain (CAD; also known as vasostatin), the N-terminal domain of calreticulin, comprising amino acids 1-180, is a potent endogenous inhibitor of angiogenesis[5]. Recombinant CAD has been shown to inhibit basic fibroblast growth factor (bFGF)- or VEGF-induced angiogenic responses of human endothelial cells[6-8] by preventing attachment of endothelial cells to laminin, thus reducing the angiogenic responses of endothelial cells[9]. CAD also has anti-inflammatory properties, which potentiates its antiangiogenic effects by limiting inflammation-driven angiogenic triggers[10]. Moreover, intramuscular gene delivery or Topical application of CAD has been demonstrated to suppress corneal and choroidal neovascularization in rats. Recently, we have extended these studies to identify the functional domain of CAD into a peptide fragment of 27 residues, CAD-like peptide 27 (CAD27), which consists of residues 137-163 of calreticulin. In this study, we investigate the anti-angiogenic effect and therapeutic efficacy of CAD27 *in vitro* and *in vivo* in a rat model of laser-induced CNV via

 doi:10.20944/preprints201807.0347.v1

85 intravitreal administration and topical application.

86

Preprints (www.preprints.org) | NOT PEER-REVIEWED | Posted: 19 July 2018 doi:10.20944/preprints201807.0347.v1

RESULTS

CAD27 inhibits the angiogenic activity of endothelial cells *in vitro* and vascular sprouting from rat aortic ring *ex vivo.*

The CAD27 peptide was manufactured by de novo synthesis for *in vitro* and *in vivo* studies (Figure 1A). To evaluate the anti-angiogenic activity of CAD27 peptides, endothelial tube formation, migration and rat aortic ring assay were performed. Compared with vehicle (% of lumen count: 100% [95% CI: 96.97-103.03], n=4) or Csr27-treated cells (Csr27 10 μg/mL: 92.56% [95% CI: 87.57-97.55] and Csr27 20 μg/mL: 99.59% [95% CI: 97.09-102.09]), cells treated with CAD27 (CAD27 10 μg/mL: 17.36% [95% CI: 12.81-21.90, n=4] and CAD27 20 μg/mL: 1.65% [95% CI: 0.13-3.17], n=4) showed a significant decrease in their capacity to form tube-like networks on Matrigel (Figure 1B). Additionally, CAD27-treated cells also showed poorer migration in the boyden's chamber migration assay (number of migrated cells in vehicle: 134 [95% CI: 117.1-150.9], Csr27 10 μg/mL: 116 [95% CI: 99.8-132.8], or Csr27 20 μg/mL: 123 [95% CI: 119.1-126.9] compared with CAD27 10 μg/mL: 77 [95% CI: 65.2-89.4] or CAD27 20 μg/mL: 67 [95% CI: 57.3-76.7], n = 3-4; Figure 1C).

To further validate the anti-angiogenic function of CAD27 *ex vivo*, the rat aortic rings were embedded in Matrigel to assess microvascular sprouting. A significant reduction of vessel sprouting from aortic ring was found in the CAD27-treated group (% of sprouting length: 12.2% [95% CI: 10.92, 13.54], n=5) compared to the vehicle- (100% [95% CI: 93.26-106.74], n=5) or Csr27-treated group (89.7% [95% CI: 87.97-91.43], n=5; Figure 2).

Effect of intravitreal or topical delivery of CAD27 on retinal function in the rat retina

To determine whether employment of CAD27 affects retinal safety, we examined retinal function with ERG on day 9 after CAD27treatments. There was no statistical difference in the latency and amplitude of the a-wave and b-wave in the eyes with intravitreal injection or topical application of CAD27 compared with the eyes-treated with vehicle or Lucentis (n=12; Table1). These results

Preprints (www.preprints.org) | NOT PEER-REVIEWED | Posted: 19 July 2018 doi:10.20944/preprints201807.0347.v1

indicated that there was no obvious retinal toxicity after intravitreal injection and topical application of CAD27.

Intravitreal and topical delivery of CAD27 alleviates laser-induced CNV lesions in rats

A rat model of laser-induced CNV was employed to evaluate the therapeutic potential of intravitreal and topical delivery of CAD27. One day after the laser surgery, CAD27 was administered via a single intravitreal injection or daily topical application (three times a day) in the CNV rats. The extent of choroidal vascularization was examined using fundus fluorescein angiography and choroidal flat-mounts with FITC-dextran perfusion on 24 and 28 days respectively after CNV induction (Figure 3). Compared with vehicle-treated eyes (60% of the eyes had score 3, 33% had score 2, and 7% had score 1, n=42), intravitreal injection of CAD27 (10 μg CAD27: 11% of the eyes had score 3, 52% had score 2, and 37% had score 1, n=27; 20 μg CAD27: 2% of the eyes had score 3, 43% had score 2, and 55% had score 1, n=40) and Lucentis (8% of the eyes had score 3, 46% had score 2, and 46% had score 1, n=26) reduced CNV score measured by FFA on day 24 (Figure 4). Similarly, the daily topical application of CAD27 also reduced the CNV score (10 μg/mL CAD27: 2% of the eyes had score 3, 58% had score 2, and 40% had score 1, n=46; 20 μg/mL CAD27: 3% of the eyes had score 3, 30% had score 2, and 67% had score 1, n=44; Figure 4).

To further confirm the therapeutic potential of CAD27, the size of CNV lesion was measured using flat-mount analysis after perfusion with FITC-dextran on day 28 (Figure 5). Compared with vehicle-treated eyes (CNV size: 82867 [95% CI: 73303-92430] μm^2, n=30), a significant reduction in the size of CNV lesion was found in the rat eyes that had received an intravitreal administration of CAD27 (CAD27 10μg: 66714 [95% CI: 61640-71787] μm^2, n=31 and CAD27 20μg: 64327 [95% CI: 59738-68915] μm^2, n=23) and Lucentis (62233 [95% CI: 56256-68209] μm^2, n=30) as well as daily topical application of CAD27 (CAD27 10μg/mL: 67959 [95% CI: 63425-72492] μm^2, n=26 and CAD27 20μg/mL: 55911 [95% CI: 48519-63302] μm^2, n=26; Figure 5). These results indicated that intravitreal and topical application of CAD27 attenuated the severity of experimental CNV.

Preprints (www.preprints.org) | NOT PEER-REVIEWED | Posted: 19 July 2018 doi:10.20944/preprints201807.0347.v1

DISCUSSION

The present study demonstrated that the de novo synthetic CAD27 peptides can inhibit angiogenesis *in vitro*, *ex vivo* and suppress ocular neovascularization in a rat model of laser-induced CNV *in vivo*. Specifically, we have confirmed the anti-angiogenic activity of CAD27 by inhibition of endothelial tube formation and migration, as well as the vascular sprouting from rat aortic ring. In addition, intravitreal and topical application of CAD27 attenuated laser-induced CNV in rats as revealed by using FFA and choroidal flat-mount, and no detectable adverse effects on retinal function was found.

CAD27 is a novel angiogenesis inhibitor derived from CAD (also known as vasostatin) [5, 6, 11] and has the potential to be superior to previously identified angiogenesis inhibitors are derived from fragments of endogenous precursor proteins as well as current therapeutic approaches (e.g. anti-VEGF antibody injections). For instance, 1) CAD27 is a much smaller, soluble and stable molecule that specifically targets endothelial cells with low toxicity[7, 12, 13], which makes it well suitable for eyedrop formulation; 2) CAD also has anti-inflammatory properties, which will help to control inflammation, a major contributor to the ongoing drive for neovascularization in nAMD[10]; 3) The effective dose of CAD for angiogenesis inhibition *in vivo* is 4-10 fold lower than that of other endogenous inhibitor such as endostatin or angiostatin[14, 15]; 4) CAD also appears to be a potent inhibitor of new vessel formation, blocking endothelial cell growth and leaving quiescent blood vessels intact[11, 16]. Thus, it was consistent with our data that CAD27 could exert its anti-angiogenic effect in the endothelial tube formation and migration assay as well as in *ex vivo* rat aortic ring assay.

Intravitreal and topical routes were used to assess the therapeutic effect of CAD27 for treatment of CNV. Intravitreal injection has been considered as an effective way to administer pharmacological treatments to the eye for managing pathological conditions associated with abnormal blood vessel growth, such as nAMD, diabetic retinopathy and which requires frequent intravitreal injections for life. Nevertheless, retinal specialists are not easily accessible in regional communities, less developed or developing countries for intraocular injections that the diseases will eventually progress

Preprints (www.preprints.org) | NOT PEER-REVIEWED | Posted: 19 July 2018 doi:10.20944/preprints201807.0347.v1

to blindness. Intravitreal injection also carries risks of potential blinding complications and serious intraocular infections. Topical application of ophthalmic formulation, is the most convenient, safe, effective and less invasive drug delivery method, could potentially eliminate the risks of eye injections and increase the accessibility for patients. Several studies have previously demonstrated the feasibility of topical application of ophthalmic formulation for management of CNV[17-20]. Therefore, in present study we have assessed the therapeutic potential of CAD27 on targeting CNV delivered via both intravitreal injection and topical application. Indeed, our data indicates both delivery routes provided similar benefits in reducing choroidal neovascular lesions, suggesting that both the drug delivery methods are available and effectual in rat lased-induced models. This data also consistence with our previous study that topical delivery of recumbent CAD proteins (CAD180 and 48) attenuates the development of CNV in rat model of laser-induced CNV[12, 21, 22]. In addition, CAD27 might have additional benefits than CAD180 or 48 as it can be chemically synthesized and low molecular weight that allows to have better retinal or trans-scleral penetration to posterior segment when it is administered through intravitreal injection and topical application, respectively. However, further study needs to be performed to confirm its pharmacokinetic profile and bioavailability in the eyes.

In summary, our study demonstrates that therapeutic delivery of CAD27 attenuates the formation of CNV *in vivo*. Although further investigations are required to assess pharmacokinetic profile and long-term efficacy, our data suggest that topical application of CAD27 may be a viable therapeutic alternative for choroidal neovascularization, as it doesn't require ocular injection and can thus avoid the risks associated with the frequent injections required for current therapies.

Preprints (www.preprints.org) | NOT PEER-REVIEWED | Posted: 19 July 2018 doi:10.20944/preprints201807.0347.v1

MATERIALS AND METHODS

Preparation of CAD27 peptide

CAD27 peptide (CGPGTKKVHVIFNYKGKNVLINKDIRC) and presumed non-functional form scrambled peptide (Csr27; CVKIGLRGNTVKPYKFNIKDHVGKNIC) were manufactured by de novo peptide synthesis (Kelowan Incs, Taipei, Taiwan). The synthesized peptides were reconstituted in Dulbecco's Phosphate Buffered Saline (DPBS; catalog no. 14190144, Gibco™, Invitrogen, Carlsbad, CA, USA) for *in vitro* and *in vivo* studies.

Cell culture

Human umbilical vein endothelial cell line, EA.hy926, were purchased from ATCC (CRL-2922™) and cultured in Dulbecco's Modified Eagle's Medium (DMEM; catalog no. 11965118, Invitrogen) supplemented with Penicillin-Streptomycin (50 U/mL; catalog no. 15140122, Invitrogen), 10% fetal bovine serum (FBS; Gibco™, Invitrogen) and L-glutamine (2mM; catalog no. 25030081, Invitrogen) in a humidified 5% CO_2 at 37℃.

Tube formation assay

Quantification of tube formation was performed using a previously described method[21] . Briefly, 24-well plate was pre-incubated with BD Matrigel™ Basement Membrane Matrix (catalog no. 356234, BD Biosciences, Franklin Lakes, NJ, USA) at 37 ℃ for 30 minutes. EA.hy926 cells were incubated with DPBS, CAD27 (10 and 20 μg/mL), or Csr27 (10 and 20 μg/mL) at 37 ℃ for 5 hours. Cells (1.5×10^4) were re-suspended in the completed medium and loaded on the top of the Matrigel. Following a 6 hours incubation at 37 ℃, each well was photographed under a bright field phase contrast microscope. The numbers of endothelial tube lumens were counted in three replicate wells and only the completed ring structures created by 3 to 5 endothelial cells were considered as tubes. The analysis was performed in Image J version 1.48 software (http://imag ej.nih.gov/ij/; provided in the National Institutes of Health, Bethesda, MD, USA).

Preprints (www.preprints.org) | NOT PEER-REVIEWED | Posted: 19 July 2018 doi:10.20944/preprints201807.0347.v1

214

215 **Cell migration assay**

216 Cell migration was performed in a Boyden's chambers (catalog no. CBA-100-C, Cell Biolabs, INC,
217 CA, USA), which comprising the upper and lower system separated by a 0.005 % gelatin coating
218 8-µm pore size polycarbonate membrane, as previously described (PMID: 20454694). EA.hy926
219 cells (2×10^4) were re-suspended in serum-free medium, loaded onto the upper well and incubated
220 with vehicle (DPBS), CAD27 (10 and 20 µg/mL), or Csr27 (10 and 20 µg/mL), respectively, in a
221 humidified 5% CO_2 at 37℃ for 6 hours. The cells on the upper side of the filter were removed. Those
222 that had migrated to the lower side were fixed in absolute methanol, stained with 10 % Giemsa
223 solution (Merck, Darmstadt, Germany) and five high power fields from each well were counted
224 under a bright field phase contrast microscope (Olympus BX40; Olympus Optical Co., Tokyo,
225 Japan).

226

227 **Aortic ring assay**

228 This *ex vivo* aortic ring angiogenesis assay was performed as described previously[21] . Briefly, the
229 thoracic aortas were excised from 3 week-old male Sprague-Dawley rats and immediately placed
230 into prechilled DMEM containing 10% FBS. Clotted blood inside the aorta was flushed with media,
231 and the peri-adventitial fibroadipose tissue was removed. Aortas were then cut into cross-sectional
232 rings about 1-1.5 mm in length. Rings were placed into a 24-well plate containing 0.5 mL of cold BD
233 Matrigel™ Basement Membrane Matrix supplemented with MCDB131 medium (catalog no.
234 10372019, Invitrogen) and incubated at 37 ℃ until the Matrigel polymerized. Subsequently, aortic
235 rings were treated with vehicle (DPBS), CAD27 (10 µg/mL), or Csr27 (10 µg/mL) and maintained in
236 a humidified 5 % CO_2 at 37℃ for 5 days. Microvascular sprouting from each aortic ring were
237 examined and imaged daily under a bright field phase contrast microscope (Olympus BX40). The
238 greatest distances from the aortic ring body to the end of the vascular sprouts (sprout length) were

Preprints (www.preprints.org) | NOT PEER-REVIEWED | Posted: 19 July 2018 doi:10.20944/preprints201807.0347.v1

239 measured by Image J version 1.48 software at 3 distinct points per ring and in 3 different rings per
240 treatment group.
241
242 **Animal and ethical approval**
243 All animals were handled in accordance with the ARVO Statement for the Use of Animals in
244 Ophthalmic and Vision Research. for the experiments performed in this study was obtained from the
245 Institutional Animal Care and Use Committee (IACUC) of Kaohsiung Veterans General Hospital.
246 The pigmented Brown Norway rats (8 week-old, female) and Sprague-Dawley rats (3 week-old,
247 male) were purchased from National Animal Center, Taipei, Taiwan. Rats were housed in standard
248 cages, with free access to food and water in a temperature-controlled environment under a 12-h light
249 (50 lux illumination) and 12-h dark (< 10 lux illumination) cycle to minimize possible light-induced
250 damage to the eye.
251
252 **Generation of CNV by laser photocoagulation**
253 The CNV lesions were induced in rat eyes by laser photocoagulation as previously described[21].
254 Briefly, Brown Norway rats were anesthetized with an intramuscular injection of a mixture of 2%
255 xylocaine (0.15 mL/kg body weight, Astra, Astra Sodertalje, Sweden) and ketamine (50 mg/kg body
256 weight, Parke-Davis, Morris Plains, NJ, USA). Pupils were dilated with 1% tropicamide (Alcon
257 Laboratories, Fort Worth, TX, USA). A piece of cover glasses was served as a contact lens to
258 improve the visibility of the fundus. Argon laser (Novus Omni; Coherent, Palo Alto, CA, USA)
259 irradiation was delivered through a slit lamp (Carl Zeiss, Oberkochen, Germany). Laser parameters
260 were set as follows: spot size of 50 μm, power of 400 mW, and exposure duration of 0.05 second.
261 Disruption of Bruch's membrane was detected by the emergence of a bubble at the center of
262 photocoagulation in the laser spotted zone. Six lesions were generated in each eye at the 1, 3, 5, 7, 9
263 and 11 o'clock positions located at equal distances from the optic disk and between the major retinal
264 vessels.

Preprints (www.preprints.org) | NOT PEER-REVIEWED | Posted: 19 July 2018 doi:10.20944/preprints201807.0347.v1

265

266 **Intravitreal injection and topical application**

267 One day after laser-induced CNV induction, rats were anesthetized with a combination of xylocaine
268 (0.15 mL/kg body weight) and ketamine (50 mg/kg body weight). Intravitreal injection was
269 performed under a surgical microscope as previously described[23] . After a small puncture through
270 the conjunctiva and sclera was created using a 30 gauge needle, a 32 gauge blunt needle connected to
271 a 10-μL Hamilton syringe was inserted into the vitreous and 5 μL of DPBS suspension containing
272 Lucentis® (ranibizumab, 50 μg; Novartis, Basel, Switzerland), CAD27 (10 and 20 μg), or vehicle
273 (DPBS) was injected into one eye of each rat using a UMP3-2 Ultra Micro Pump (World Precision
274 Instruments, Sarasota, FL, USA) at a rate of 100 nL/s. Only a single injection was permed in the
275 CNV rat. The CAD27 (10 and 20 μg/mL) were formulated as eye drop in DPBS and topical installed
276 three times a day in the rat eye after CNV induction for 28 days.

277

278 **Electroretinogram (ERG)**

279 The single bright flash ERGs (UTAS-E 300; LKC Technology, Gaithersburg, MD) under a
280 dark-adapted environment (~12 hours) were performed to assess the effect of intravitreal or topical
281 administration of CAD 27 on retinal function. After at least 30 mins of darkness adaptation, rats were
282 anesthetized. Gold foil was placed on the cornea with 2% methylcellulose gel (Omni Vision,
283 Neuhausen, Switzerland). A reference electrode was attached to the shaven skin of the head and a
284 ground electrode clipped to the rat's ear. After reducing the background noise below 60 Hz, a single
285 flash of bright light (duration, 100 ms), 30 cm from the eye, was used as the light stimulus.
286 Responses were amplified with a gain setting ±500 μV and filtered with low 0.3 Hz and high 500 Hz
287 from an amplifier. Data were acquired, digitized, and analyzed using EM for Windows, version 2.6.

288

289 **Fundus fluorescein angiography (FFA)**

Preprints (www.preprints.org) | NOT PEER-REVIEWED | Posted: 19 July 2018 doi:10.20944/preprints201807.0347.v1

The size of CNV lesions were evaluated by FFA analysis using a digital fundus camera (Visupac 450, Ziess FF450, Germany) on day 24 after laser photocoagulation[24]. The rats were anaesthetized and the fluorescein sodium solution (10% Fluorescite; Alcon, Fort Worth, TX, USA) was intraperitoneally injected at a dose of 0.1 ml/kg body weight. Late-phase angiograms were obtained at 8 minutes after injection, and digital fundus pictures of bilateral eyes were taken within 1 minute. A choroidal neovascularization was defined as present when early hyper-fluorescence with late leakage was present at the site of laser injury[21]. The leakage of the CNV lesions were graded using leakage score system[25, 26]. Score 0 means no staining (no hyper-fluorescence), Score 1 means staining (hyper-fluorescence without leakage), Score 2 means moderate leakage (hyper-fluorescence in the early or midtransit images and late leakage), and Score 3 means heavy leakage (bright hyper-fluorescence in the transit images and late leakage beyond treated areas). The scores were assessed by two independent ophthalmologists who were masked to the experimental design.

Quantification of choroidal vascularity by flat-mounted analysis

Rats were euthanized 28 days after laser photocoagulation. The choroidal blood vessels in rat eyes were labeled by perfusion with fluorescein isothiocyanate (FITC)-dextran (2 x 10^6 MW; catalog no. FD2000S, Sigma-Aldrich, St. Louis, MO, USA)[27, 28]. Briefly, the rats were anaesthetized and subjected to an intracardiac perfusion of approximately 50 mL of lactated Ringer solution, followed by 20 mL of FITC-dextran in lactated Ringer solution (5 mg/mL) with gelatin (10%, w/v; catalog no. G9382, Sigma-Aldrich). The eyes were enucleated and fixed in 10% phosphate-buffered formalin for 2 hours at room temperature. After the cornea and lens were removed, the RPE/choroid/sclera flat-mounts were obtained on microscopic slides. Flat-mounts were imaged with a laser-scanning confocal fluorescence microscope. The areas of hyper-fluorescence associated with each CNV lesion was measured by observers who were blinded to the groups using ImageJ version 1.48 software.

Statistical Analysis

 doi:10.20944/preprints201807.0347.v1

316 Results are presented as means ± standard errors of the means (SEM). The experimental data was
317 analyzed with one-way ANOVA followed by Tukey's multiple comparisons test or two-tailed
318 Student's t-test (GraphPad Prism software version 7.0). A value of *P* less than 0.05 was considered
319 statistically significant.
320

ACKNOWLEDGEMENTS

This work was supported by grants from the Kaohsiung Veterans General Hospital (VGHKS 101-056, 103-089), The National Health and Medical Research Council of Australia (#1061912), The Ophthalmic Research Institute of Australia, and The Rebecca L. Cooper Medical Research Foundation.

AUTHOR CONTRIBUTIONS

Conceptualization, Y.S.B., M.H.T. and G.S.L. Methodology, Y.S.B., H.H., M.H.T. and G.S.L. Formal Analysis, Y.S.B., J.C., P.J.T., M.H.T. and G.S.L. Investigation, Y.S.B., J.C. and P.J.T. Resources, Y.S.B., S.J.S., M.H.T. and G.S.L. Data Curation, Y.S.B., M.H.T. and G.S.L. Writing- Original Draft, Y.S.B., M.H.T. and G.S.L. Writing- Review & Editing, J.C., S.J.S., H.C.L. and H.H. Visualization, Y.S.B., J.C., M.H.T. and G.S.L. Supervision, Y.S.B., M.H.T. and G.S.L. Project Administration, Y.S.B., M.H.T. and G.S.L. Funding Acquisition, Y.S.B. and M.H.T.

CONFLICTS OF INTEREST

None of the authors have conflicts of interest to disclose.

REFERENCES

1. Campochiaro, P. A., Retinal and choroidal neovascularization. *J.Cell Physiol* **2000,** 184, (3), 301-310.
2. Cheung, C. M. G.; Arnold, J. J.; Holz, F. G.; Park, K. H.; Lai, T. Y. Y.; Larsen, M.; Mitchell, P.; Ohno-Matsui, K.; Chen, S. J.; Wolf, S.; Wong, T. Y., Myopic Choroidal Neovascularization: Review, Guidance, and Consensus Statement on Management. *Ophthalmology* **2017,** 124, (11), 1690-1711.
3. Chan, W. M.; Lai, T. Y.; Liu, D. T.; Lam, D. S., Intravitreal bevacizumab (Avastin) for myopic choroidal neovascularization: six-month results of a prospective pilot study. *Ophthalmology* **2007,** 114, (12), 2190-6.
4. Ip, M. S.; Scott, I. U.; Brown, G. C.; Brown, M. M.; Ho, A. C.; Huang, S. S.; Recchia, F. M.; American Academy of, O., Anti-vascular endothelial growth factor pharmacotherapy for age-related macular degeneration: a report by the American Academy of Ophthalmology. *Ophthalmology* **2008,** 115, (10), 1837-46.
5. Pike, S. E.; Yao, L.; Jones, K. D.; Cherney, B.; Appella, E.; Sakaguchi, K.; Nakhasi, H.; Teruya-Feldstein, J.; Wirth, P.; Gupta, G.; Tosato, G., Vasostatin, a calreticulin fragment, inhibits angiogenesis and suppresses tumor growth. *The Journal of experimental medicine* **1998,** 188, (12), 2349-56.
6. Pike, S. E.; Yao, L.; Setsuda, J.; Jones, K. D.; Cherney, B.; Appella, E.; Sakaguchi, K.; Nakhasi, H.; Atreya, C. D.; Teruya-Feldstein, J.; Wirth, P.; Gupta, G.; Tosato, G., Calreticulin and calreticulin fragments are endothelial cell inhibitors that suppress tumor growth. *Blood* **1999,** 94, (7), 2461-8.
7. Wu, P. C.; Yang, L. C.; Kuo, H. K.; Huang, C. C.; Tsai, C. L.; Lin, P. R.; Wu, P. C.; Shin, S. J.; Tai, M. H., Inhibition of corneal angiogenesis by local application of vasostatin. *Molecular vision* **2005,** 11, 28-35.
8. Shu, Q.; Li, W.; Li, H.; Sun, G., Vasostatin inhibits VEGF-induced endothelial cell proliferation, tube formation and induces cell apoptosis under oxygen deprivation. *International journal of molecular sciences* **2014,** 15, (4), 6019-30.
9. Yao, L.; Pike, S. E.; Tosato, G., Laminin binding to the calreticulin fragment vasostatin regulates endothelial cell function. *Journal of leukocyte biology* **2002,** 71, (1), 47-53.
10. Huegel, R.; Velasco, P.; De la Luz Sierra, M.; Christophers, E.; Schroder, J. M.; Schwarz, T.; Tosato, G.; Lange-Asschenfeldt, B., Novel anti-inflammatory properties of the angiogenesis inhibitor vasostatin. *J Invest Dermatol* **2007,** 127, (1), 65-74.
11. Yao, L.; Pike, S. E.; Setsuda, J.; Parekh, J.; Gupta, G.; Raffeld, M.; Jaffe, E. S.; Tosato, G., Effective targeting of tumor vasculature by the angiogenesis inhibitors vasostatin and interleukin-12. *Blood* **2000,** 96, (5), 1900-5.
12. Sheu, S. J.; Chou, L. C.; Bee, Y. S.; Chen, J. F.; Lin, H. C.; Lin, P. R.; Lam, H. C.; Tai, M. H., Suppression of choroidal neovascularization by intramuscular polymer-based gene delivery

of vasostatin. *Exp Eye Res* **2005,** 81, (6), 673-9.

13. Lange-Asschenfeldt, B.; Velasco, P.; Streit, M.; Hawighorst, T.; Pike, S. E.; Tosato, G.; Detmar, M., The angiogenesis inhibitor vasostatin does not impair wound healing at tumor-inhibiting doses. *J Invest Dermatol* **2001,** 117, (5), 1036-41.

14. O'Reilly, M. S.; Boehm, T.; Shing, Y.; Fukai, N.; Vasios, G.; Lane, W. S.; Flynn, E.; Birkhead, J. R.; Olsen, B. R.; Folkman, J., Endostatin: an endogenous inhibitor of angiogenesis and tumor growth. *Cell* **1997,** 88, (2), 277-85.

15. O'Reilly, M. S.; Holmgren, L.; Chen, C.; Folkman, J., Angiostatin induces and sustains dormancy of human primary tumors in mice. *Nat Med* **1996,** 2, (6), 689-92.

16. Sheu, S. J.; Bee, Y. S.; Ma, Y. L.; Liu, G. S.; Lin, H. C.; Yeh, T. L.; Liou, J. C.; Tai, M. H., Inhibition of choroidal neovascularization by topical application of angiogenesis inhibitor vasostatin. *Molecular vision* **2009,** 15, 1897-905.

17. Birke, K.; Lipo, E.; Birke, M. T.; Kumar-Singh, R., Topical application of PPADS inhibits complement activation and choroidal neovascularization in a model of age-related macular degeneration. *PloS one* **2013,** 8, (10), e76766.

18. Cloutier, F.; Lawrence, M.; Goody, R.; Lamoureux, S.; Al-Mahmood, S.; Colin, S.; Ferry, A.; Conduzorgues, J. P.; Hadri, A.; Cursiefen, C.; Udaondo, P.; Viaud, E.; Thorin, E.; Chemtob, S., Antiangiogenic activity of aganirsen in nonhuman primate and rodent models of retinal neovascular disease after topical administration. *Investigative ophthalmology & visual science* **2012,** 53, (3), 1195-203.

19. Kiuchi, K.; Matsuoka, M.; Wu, J. C.; Lima e Silva, R.; Kengatharan, M.; Verghese, M.; Ueno, S.; Yokoi, K.; Khu, N. H.; Cooke, J. P.; Campochiaro, P. A., Mecamylamine suppresses Basal and nicotine-stimulated choroidal neovascularization. *Investigative ophthalmology & visual science* **2008,** 49, (4), 1705-11.

20. Robbie, S. J.; Lundh von Leithner, P.; Ju, M.; Lange, C. A.; King, A. G.; Adamson, P.; Lee, D.; Sychterz, C.; Coffey, P.; Ng, Y. S.; Bainbridge, J. W.; Shima, D. T., Assessing a novel depot delivery strategy for noninvasive administration of VEGF/PDGF RTK inhibitors for ocular neovascular disease. *Investigative ophthalmology & visual science* **2013,** 54, (2), 1490-500.

21. Bee, Y. S.; Sheu, S. J.; Ma, Y. L.; Lin, H. C.; Weng, W. T.; Kuo, H. M.; Hsu, H. C.; Tang, C. H.; Liou, J. C.; Tai, M. H., Topical application of recombinant calreticulin peptide, vasostatin 48, alleviates laser-induced choroidal neovascularization in rats. *Molecular vision* **2010,** 16, 756-67.

22. Wu, P. C.; Yang, L. C.; Kuo, H. K.; Huang, C. C.; Tsai, C. L.; Lin, P. R.; Shin, S. J.; Tai, M. H., Inhibition of corneal angiogenesis by local application of vasostatin. *Molecular vision* **2005,** 11, 28-35.

23. Tu, L.; Wang, J. H.; Barathi, V. A.; Prea, S. M.; He, Z.; Lee, J. H.; Bender, J.; King, A. E.; Logan, G. J.; Alexander, I. E.; Bee, Y. S.; Tai, M. H.; Dusting, G. J.; Bui, B. V.; Zhong, J.; Liu,

 doi:10.20944/preprints201807.0347.v1

G. S., AAV-mediated gene delivery of the calreticulin anti-angiogenic domain inhibits ocular neovascularization. *Angiogenesis* **2018,** 21, (1), 95-109.

24. Sheu, S. J.; Chou, L. C.; Bee, Y. S.; Chen, J. F.; Lin, H. C.; Lin, P. R.; Lam, H. C.; Tai, M. H., Suppression of choroidal neovascularization by intramuscular polymer-based gene delivery of vasostatin. *Experimental Eye Research* **2005,** 81, (6), 673-679.

25. Rich, R. M.; Rosenfeld, P. J.; Puliafito, C. A.; Dubovy, S. R.; Davis, J. L.; Flynn, H. W., Jr.; Gonzalez, S.; Feuer, W. J.; Lin, R. C.; Lalwani, G. A.; Nguyen, J. K.; Kumar, G., Short-term safety and efficacy of intravitreal bevacizumab (Avastin) for neovascular age-related macular degeneration. *Retina* **2006,** 26, (5), 495-511.

26. Lai, C. C.; Wu, W. C.; Chen, S. L.; Xiao, X.; Tsai, T. C.; Huan, S. J.; Chen, T. L.; Tsai, R. J.; Tsao, Y. P., Suppression of choroidal neovascularization by adeno-associated virus vector expressing angiostatin. *Investigative ophthalmology & visual science* **2001,** 42, (10), 2401-7.

27. Edelman, J. L.; Castro, M. R., Quantitative image analysis of laser-induced choroidal neovascularization in rat. *Exp Eye Res* **2000,** 71, (5), 523-33.

28. Nambu, H.; Nambu, R.; Melia, M.; Campochiaro, P. A., Combretastatin A-4 phosphate suppresses development and induces regression of choroidal neovascularization. *Invest Ophthalmol.Vis.Sci.* **2003,** 44, (8), 3650-3655.

 doi:10.20944/preprints201807.0347.v1

433 **TABLE**

434 **Table 1. The effect of intravitreal and topical application of CAD27 on retinal function assessed by ERG.**

435

ERG parameters	Vehicle	Lucentis (IVI)	CAD27 (10μg, IVI)	CAD27 (20μg, IVI)	CAD27 (10μg/mL, TA)	CAD27 (20μg/mL, TA)	P value
a-wave amplitude, μV	168.4±14.06	161.4±28.33	150.3±21.1	159.4±23.2	150.5±20.28	138.9±23.04	0.088
a-wave latency, ms	19.81±1.36	19.24±1.93	18.15±3.00	19.82±2.99	18.47±2.53	19.38±2.20	0.449
b-wave amplitude μV	328.5±54.51	310.4±35.42	306.6±65.77	275.2±67.29	303.7±30.79	289.3±47.63	0.306
b-wave latency, ms	60.2±4.55	58.25±6.72	54.1±4.84	53.75±3.24	57.41±5.98	57.83±5.23	0.062

436

437 Statistical analysis was performed using one-way ANOVA.

438 IVI: intravitreal injection, TA: topical application.

Preprints (www.preprints.org) | NOT PEER-REVIEWED | Posted: 19 July 2018 doi:10.20944/preprints201807.0347.v1

FIGURE LEGEND

Figure 1. The effect of CAD27 on *in vitro* angiogenic activities. (A) Schematic representation of CAD27. CAD27 was derived from anti-angiogenic domain (residues 137-163) of calreticulin. (B) and (C) Effect of CAD27 on tube formation and migration in human endothelial cells (EA.hy926) was assessed. (B) Representative images and quantitative analysis of tube formation assay characterizing the lumen formation, and data are presented as the mean ± SEM (n=4). (C) Representative images and quantification of migration assay characterizing migrated cells, and data are presented as the mean ± SEM (n=3-4). Statistical analysis between groups was performed using one-way ANOVA followed by Tukey's multiple comparisons test (**$p < 0.001$).

Figure 2. The effect of CAD27 on vascular sprouting from rat aortic ring explants. (A) Representative images and (B) quantitative analysis of vascular sprouting in 3 week-old rat aortic ring explants. Data are presented as the mean ± SEM (n=5). Statistical analysis between groups was performed using one-way ANOVA followed by Tukey's multiple comparisons test (**$p < 0.001$). Red lines indicated the border zone of vascular sprouting.

Figure 3. A schematic diagram of the timeline for the laser-induced CNV rat model, treatments and examination. Choroidal vascularity of laser-induced CNV lesions was examined by FFA (day 24) and choroidal flat-mount labeling with FITC-dextran (day 28) after a single intravitreal injection or daily topical application of CAD27.

Figure 4. Fluorescein angiographic analysis of CNV lesions after an intravitreal or daily topical application of CAD27. Laser-induced CNV lesions was examined by fundus fluorescein angiography. (A) Representative CNV lesions in rat eyes were identified by fundus fluorescein angiography after an intravitreal or daily topical application of CAD27. (B) CNV lesions from fluorescein angiography were analyzed at days 24 after treatment, and data are presented as

Preprints (www.preprints.org) | NOT PEER-REVIEWED | Posted: 19 July 2018 doi:10.20944/preprints201807.0347.v1

465 percentage of CNV score (n=26-46 from 6-8 eyes). Yellow arrows indicated the lesions of CNV. Lu:
466 Lucentis, IVI: intravitreal injection, TA: topical application.
467
468 **Figure 5. Flat-mount analysis of choroidal vascularity after an intravitreal or daily topical**
469 **application of CAD27.** Choroidal vascularity of laser-induced CNV lesions was examined by
470 labeling using FITC-dextran. (A) Representative profile of FITC-dextran-positive blood vessels in
471 choroidal flat-mounts at day 28 after treatment. (B) FITC-dextran labeling CNV in the choroidal
472 flat-mounts was quantified and data are presented as mean ± SEM (n=26-31 from 6-8 eyes).
473 Statistical analysis between groups was performed using two-tailed Student's t-test (*$p < 0.05$, **$p <$
474 0.001, ***$p < 0.0001$). Red lines indicated the lesions of CNV in choroid flat-mount. Lu: Lucentis,
475 IVI: intravitreal injection, TA: topical application.
476

Preprints (www.preprints.org) | NOT PEER-REVIEWED | Posted: 19 July 2018 doi:10.20944/preprints201807.0347.v1

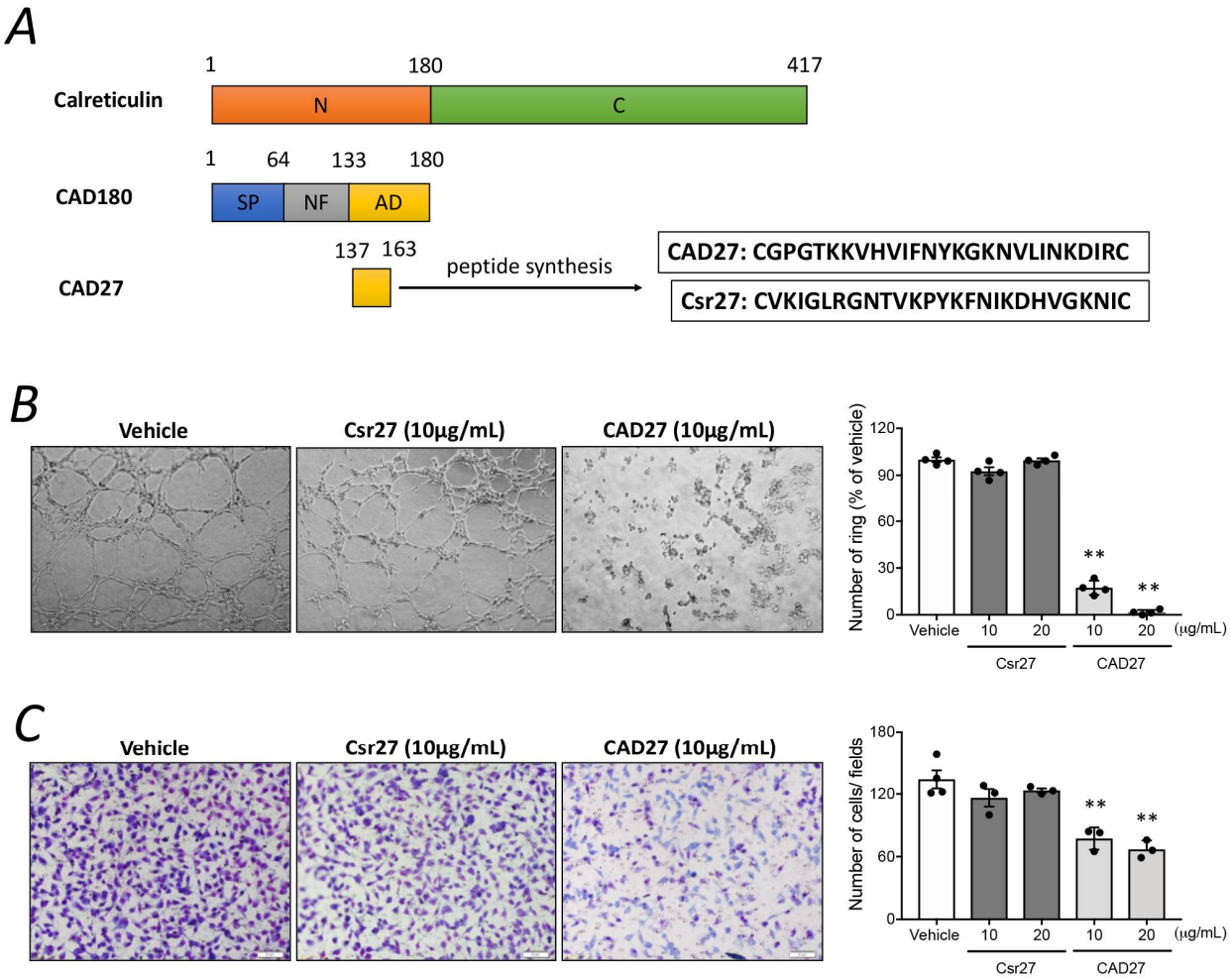

Figure 1. The effect of CAD27 on *in vitro* angiogenic activities. (A) Schematic representation of CAD27. CAD27 was derived from anti-angiogenic domain (residues 137-163) of calreticulin. (B) and (C) Effect of CAD27 on tube formation and migration in human endothelial cells (EA.hy926) was assessed. (B) Representative images and quantitative analysis of tube formation assay characterizing the lumen formation, and data are presented as the mean ± SEM (n=4). (C) Representative images and quantification of migration assay characterizing migrated cells, and data are presented as the mean ± SEM (n=3-4). Statistical analysis between groups was performed using one-way ANOVA followed by Tukey's multiple comparisons test (**$p < 0.001$).

Preprints (www.preprints.org) | NOT PEER-REVIEWED | Posted: 19 July 2018 doi:10.20944/preprints201807.0347.v1

489

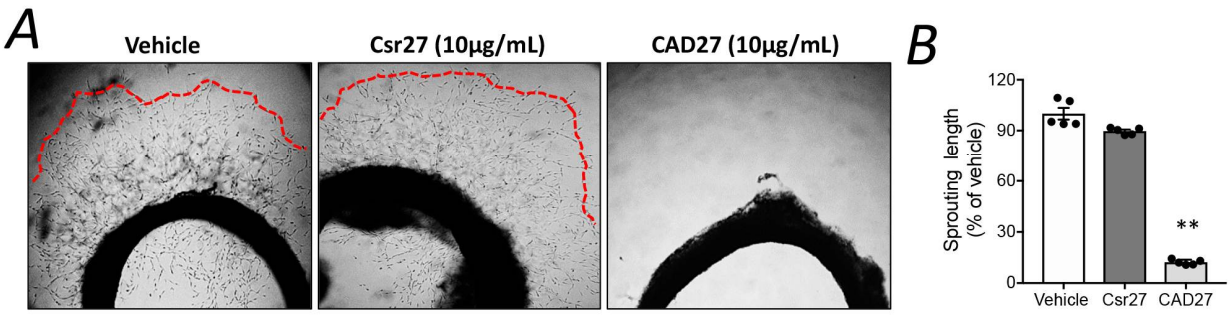

490

491 **Figure 2. The effect of CAD27 on vascular sprouting from rat aortic ring explants.** (A)
492 Representative images and (B) quantitative analysis of vascular sprouting in 3 week-old rat aortic
493 ring explants. Data are presented as the mean ± SEM (n=5). Statistical analysis between groups was
494 performed using one-way ANOVA followed by Tukey's multiple comparisons test (**$p < 0.001$).
495 Red lines indicated the border zone of vascular sprouting.

496

Preprints (www.preprints.org) | NOT PEER-REVIEWED | Posted: 19 July 2018 doi:10.20944/preprints201807.0347.v1

497

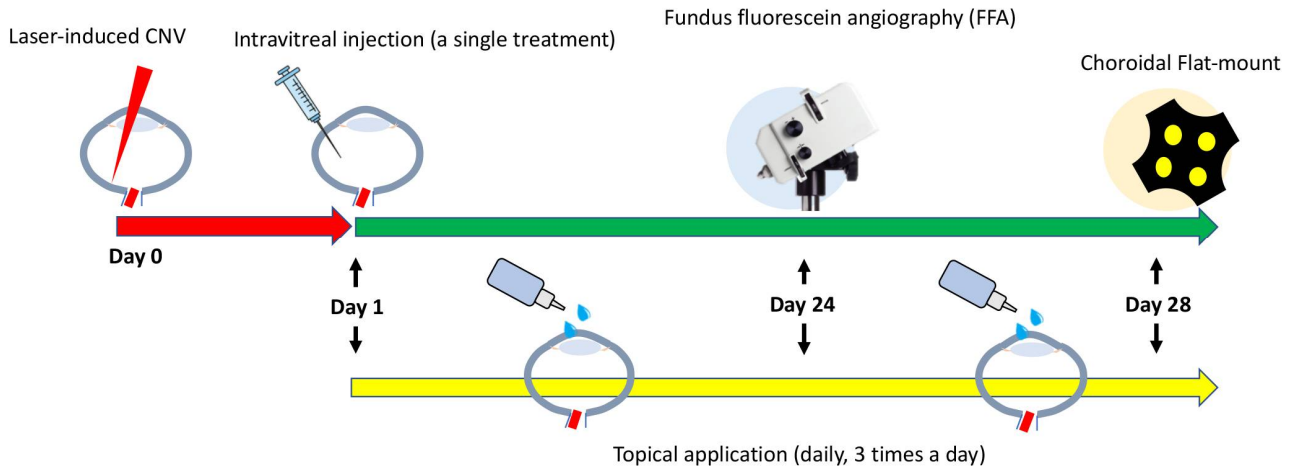

498

499 **Figure 3. A schematic diagram of the timeline for the laser-induced CNV rat model, treatments**
500 **and examination.** Choroidal vascularity of laser-induced CNV lesions was examined by FFA (day
501 24) and choroidal flat-mount labeling with FITC-dextran (day 28) after a single intravitreal injection
502 or daily topical application of CAD27.

503

504

Preprints (www.preprints.org) | NOT PEER-REVIEWED | Posted: 19 July 2018 doi:10.20944/preprints201807.0347.v1

505

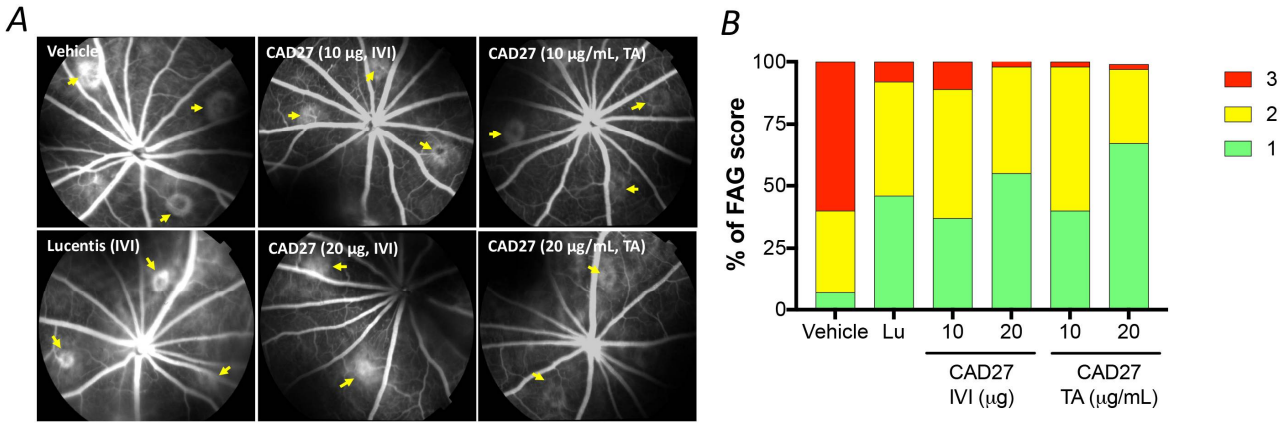

506

507 **Figure 4. Fluorescein angiographic analysis of CNV lesions after an intravitreal or daily topical**
508 **application of CAD27.** Laser-induced CNV lesions was examined by fundus fluorescein
509 angiography. (A) Representative CNV lesions in rat eyes were identified by fundus fluorescein
510 angiography after an intravitreal or daily topical application of CAD27. (B) CNV lesions from
511 fluorescein angiography were analyzed at days 24 after treatment, and data are presented as
512 percentage of CNV score (n=26-46 from 6-8 eyes). Yellow arrows indicated the lesions of CNV. Lu:
513 Lucentis, IVI: intravitreal injection, TA: topical application.

514

Preprints (www.preprints.org) | NOT PEER-REVIEWED | Posted: 19 July 2018 doi:10.20944/preprints201807.0347.v1

515

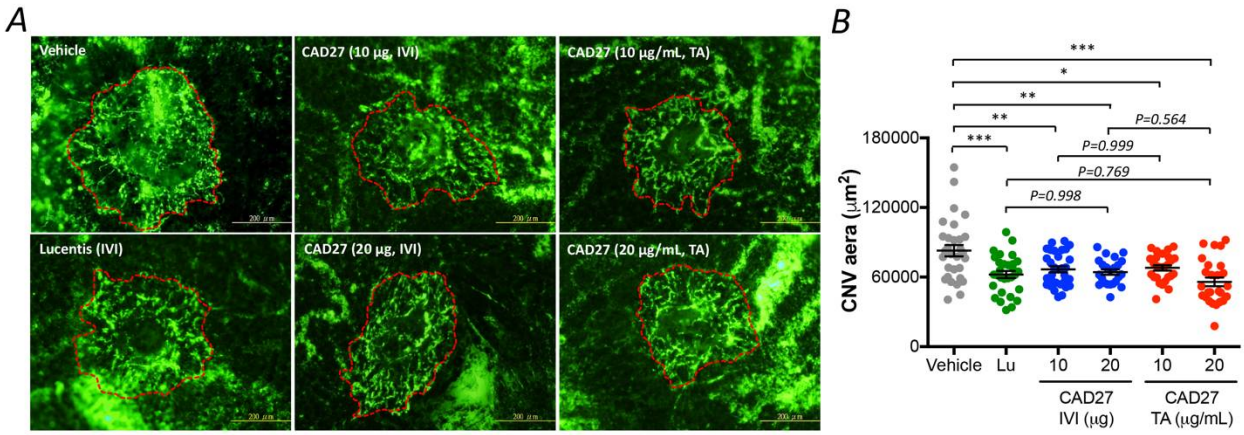

516

517 **Figure 5. Flat-mount analysis of choroidal vascularity after an intravitreal or daily topical**
518 **application of CAD27.** Choroidal vascularity of laser-induced CNV lesions was examined by
519 labeling using FITC-dextran. (A) Representative profile of FITC-dextran-positive blood vessels in
520 choroidal flat-mounts at day 28 after treatment. (B) FITC-dextran labeling CNV in the choroidal
521 flat-mounts was quantified and data are presented as mean ± SEM (n=26-31 from 6-8 eyes).
522 Statistical analysis between groups was performed using two-tailed Student's t-test (*$p < 0.05$, **$p <$
523 0.001, ***$p < 0.0001$). Red lines indicated the lesions of CNV in choroid flat-mount. Lu: Lucentis,
524 IVI: intravitreal injection, TA: topical application.

525